Toxicity, morphological and structural properties of chitosan-coated Bi_2O_3–$Bi(OH)_3$ nanoparticles prepared via DC arc discharge in liquid: a potential nanoparticle-based CT contrast agent

Mohsen Mohammadi[1], Atiyeh Tavajjohi[1], Azin Ziashahabi[1], Negin Pournoori[2], Samad Muhammadnejad[3], Hamid Delavari[1], Reza Poursalehi[1] ✉

[1]*Department of Materials Engineering, Tarbiat Modares University, P.O. Box 14115-143, Tehran, Iran*
[2]*Department of Medical Physics and Biomedical Engineering, Tehran University of Medical Sciences, Tehran, Iran*
[3]*Biomolecular Imaging and Analysis Group, Research Center for Molecular and Cellular Imaging, Tehran University of Medical Sciences, Tehran, Iran*
✉ *E-mail: poursalehi@modares.ac.ir*

Published in Micro & Nano Letters; Received on 8th May 2018; Revised on 19th October 2018; Accepted on 13th November 2018

In this study, Bi_2O_3 nanoparticles were employed as computed tomography (CT) contrast agents. In this regard, X-ray attenuation of Bi_2O_3 nanoparticles, prepared via DC arc discharge in water, was investigated. In addition, the optical, structural, morphology and cytotoxicity properties of afforded nanoparticles were also studied. The electric arc discharge was done via bismuth electrodes in a water medium. Then, to stabilise Bi_2O_3 nanoparticles, chitosan molecule was cross linked via glutaraldehyde around Bi_2O_3 nanoparticles. X-ray diffraction analysis demonstrated the monoclinic structure and field emission-scanning electron microscopy images clarified the average size of Bi_2O_3 as 40 nm. Fourier transform infrared analysis proved chitosan band formation around Bi_2O_3 nanoparticles. The 3-(4,5-dimethylthiazol-2-yl)-2,5-diphenyltetrazolium bromide (MTT) assay revealed no considerable toxicity after 72 h. Finally, X-ray CT of chitosan-coated Bi_2O_3 nanoparticles and Iohexol was carried out at concentrations of 1–6 mg/ml. The CT number of chitosan-coated Bi_2O_3 nanoparticles measured 16, 30, 49, 66, 75 and 85, as well as, respective numbers for Iohexol were 5, 14, 25, 34, 44 and 57. Therefore, it displayed that X-ray attenuation of chitosan-coated Bi_2O_3 nanoparticle was more in comparison with Iohexol at the same concentrations. Eventually, the results demonstrated that chitosan-coated Bi_2O_3 nanoparticles are a suitable candidate for commercial iodine contrast agent substitution.

1. Introduction: To obtain high-quality images by an appropriate resolution in X-ray computed tomography (CT), contrast agents have been employed dramatically [1–3]. The most common choices as contrast agents are iodine molecules such as Iohexol [1, 4]. However, there are some limitations to the use of this type of contrast agent. For instance, unfavourable resolution, toxicity, fast disposal of kidneys, inability to detect some cancer molecules and sensitisation in some patients are some of the iodine molecules disadvantages as contrast agents [5, 6].

Nowadays, investigations extended to find an appropriate substitution for iodine contrast agents [3, 5, 6]. In this respect, some factors such as atomic mass, absorption coefficient, side effects, and stability were considered [7, 8]. Furthermore, the feasibility of surface modification to target certain biomarkers of disease was contemplated. In this regard, metal nanoparticles were cogitated as contrast agents because of their high absorbance coefficient and surface modification ability [2, 6]. Gold, gadolinium, ytterbium, bismuth, zirconium, tantalum, and some of their compounds such as WO_3 and Bi_2S_3 were studied as X-ray CT scan contrast agents [6, 9–16]. Although gold nanoparticles and their combinations are not toxic in specific concentration and present high-resolution images, their high daily cost is not rational for clinical applications [9, 17]. Hence, several metallic nanoparticles with high density and atomic mass were investigated and the results revealed remarkable and reliable results in comparison with gold nanoparticles [18, 19].

Bismuth nanoparticles are appropriate inorganic metallic nanoparticles to play the contrast agent role in CT scan. Bismuth nanoparticles are antimicrobial, non-toxic, and inexpensive by considerable absorbance coefficients [20, 21]. In addition, bismuth nanoparticles were employed to concentrate radiation in radiotherapy to treat cancer tumours [22, 23]. Therefore, compounds that include bismuth nanoparticles provide a suitable response to X-ray radiation in CT scan and produce appropriate high-resolution images. Furthermore, the surface functionalisation ability of bismuth nanoparticles affords several applications such as targeting biomarkers. There are rare reports of using bismuth nanoparticles elementally as a contrast agent for CT [24]. The stability of bismuth nanoparticles didn't literature notably. Besides, instability of bismuth nanoparticles in inorganic liquid mediums like water, leads to shape bismuth oxide. Therefore, bismuth compound nanoparticles usage increased dramatically [12, 25]. In this regard, most studies have been carried out on bismuth sulphide [16, 22]. In addition, to obtain images with suitable resolution, bismuth sulphide has been prepared in various routes [26, 27]. For this purpose, the most exerted method is surface modification by coating some polymeric compounds such as poly ethylene glycol and peptide [28, 29]. Beside bismuth sulphide, bismuth oxide nanoparticles are the other choice for playing the contrast agent role. Bismuth oxide nanoparticles have antimicrobial, anticancer and antifungal properties [30, 31]. In addition, bismuth oxide nanoparticles are not toxic and have extensive capacity in medicinal applications [21]. Furthermore, bismuth oxide surface modification ability leads to targeting certain biomarkers and extra functions such as multimodal imaging [32]. Hence, bismuth oxide nanoparticles can be an appropriate substitution instead of Ioxeol as a contrast agent.

In the previous studies, various methods have been employed to synthesise bismuth oxide nanoparticles including polyacrylamide gel route, solvo-thermal, citrate gel method, flame spray pyrolysis, oxidative metal vapour phase deposition and laser ablation [33, 34]. In the case of using bismuth oxide nanoparticles as a portion of contrast agents, the prevailing route is the vapour deposition method. Herein, to synthesise bismuth oxide nanoparticles, electrical arc discharge (EAD) approach has been employed in water medium. This method had been carried out to synthesis ZnO nanoparticles by Ziashahabi *et al.* [35] previously. In this regard, suitable voltage

and current were applied between bismuth oxide electrodes in water. Then, the generated plasma led to the formation of bismuth oxide nanoparticles. EAD is not a complicated method and it does not need expensive precursor and specific atmosphere conditions. Moreover, various sizes and shapes are accessible by regulating substantial factors. In addition to ZnO nanoparticles preparation, carbon nanotubes, WO_3, and gold nanoparticles have been synthesised via the EAD method [35–39].

To employ bismuth oxide nanoparticles as contrast agents, they have to stabilise uniformly in an aqueous medium to prevent nanoparticles precipitation in patient body. Various materials have been used to modify the surface of the CT contrast agents. Polyethylene glycol (PEG), glycol chitosan (GC) and heparin are some of common biocompatible modifiers [28, 29, 40]. The above- mentioned polymers allow nanoparticles to play more functions in addition to CT contrast agent role. For instance, they enable targeting biomarkers, tumour-targeting CT imaging, dual CT/optical cancer imaging, liver-specific CT imaging and multi-modal imaging [41–43]. Because of chitosan surface modification ability, it has drawn considerable attention [44, 45]. Chitosan is a polysaccharide that derives from chitin. Chitin is one of the most significant natural polymers that is the structural element in fungi cell walls and exoskeleton of crustaceans such as shrimps and crabs [46, 47]. The copious applications of chitosan in biomedical and pharmaceutical have been reported [48, 49]. The non-toxicity, biocompatibility and appropriate biodegradability of chitosan give rise to its applications in various biomedical studies such as drug delivery, haemodialysis, and artificial skin [50, 51].

To stabilise Bi_2O_3 nanoparticles for the mentioned objective, surface modification was carried out and chitosan coated to the nanoparticles surface and cross-linked by glutaraldehyde (GTA) in suitable pH. Afterwards, ultraviolet–visible (UV–vis) spectroscopy and X-ray diffraction (XRD) analysis were carried out to investigate the formation and crystalline phase of the prepared Bi_2O_3 nanoparticles. Furthermore, Fourier transform infrared (FTIR) spectroscopy of Bi_2O_3 nanoparticles employed to assess cross-linked chitosan around Bi_2O_3 nanoparticles. Then, X-ray attenuation of chitosan-coated Bi_2O_3 nanoparticles and commercial Iohexol was evaluated to compare their CT number as contrast agents. Finally, to assess the cytotoxicity of chitosan-coated Bi_2O_3 nanoparticles, MTT ((3-(4,5-dimethylthiazol-2-yl)-2,5-diphenyltetrazolium bromide) assay was carried out on the Human Dermal Fibroblasts (HDF-1) cell line. By and large, results demonstrated that chitosan-coated Bi_2O_3 nanoparticles are an appropriate choice for the X-ray CT contrast agent.

2. Materials and methods

2.1. Bi_2O_3 nanoparticles preparation: In this research, bismuth oxide nanoparticles prepared via the EAD method in water. To achieve the goal, two bismuth rods of 99.5% purity with 5 cm length and 4 mm diameter were employed. The bismuth electrodes plunged in a beaker of 400 ml deionised water and a DC power supply afforded 5 A current. In this approach, no surfactants and chemical additives were used and nanoparticles synthesised through EAD between the bismuth electrodes. By applying voltage, an explosion occurred in water between bismuth electrodes and arc discharge initiated. The generated plasma gives rise to ionisation of bismuth electrodes and water molecules. Finally, by the reaction of activated species, bismuth nanoparticles were produced. After 5 min of the EAD process, a colloidal dark solution was obtained. Owing to the instability of bismuth nanoparticles in a water medium, bismuth nanoparticles were oxidised. Hence, according to the time-dependable oxidation of bismuth nanoparticles, the solution colour changed from black to white gradually. After a week, the whole bismuth nanoparticles converted to Bi_2O_3 nanoparticles.

2.2. Chitosan coating on Bi_2O_3 nanoparticles: Forasmuch as Bi_2O_3 nanoparticles have to stabilise for clinical applications, their surface modified by linking chitosan. For this purpose, 0.2 g chitosan was dissolved completely in 10 ml deionised water with pH of 4 that is acidified by 2 ml 3 M acetic acid. The selected pH was based on the Bi_2O_3 pH-zeta potential diagram. Afterwards, the prepared chitosan solution was added to 250 ml of synthesised Bi_2O_3 nanoparticles drop-wise with a concentration of 0.5 mg/ml and stirred for 10 h. Then, to cross-link chitosan, 4 µl of GTA dissolved in 10 ml deionised water was added to the Bi_2O_3–chitosan mixture drop-wise and stirred vigorously for 5 h. To obtain the desired concentration, the prepared solution was condensed via a rotary evaporator at 80°C. Finally, chitosan coated Bi_2O_3 nanoparticles dialysed by 12 kDa dialysis bag for 3 days, to remove un-crosslinked GTA.

2.3. Characterisation: To corroborate the formation of bismuth oxide nanoparticles according to the EAD method, UV-vis spectroscopy was carried out initially. The spectroscopy was carried out via a SPUV-26 SC-Tech spectrophotometer at room temperature. XRD was used to study the crystalline and phase composition of the synthesised bismuth oxide nanoparticles via a Philips XPERT MPD system with a cobalt Kα by radiation at 1.79 Å wavelength. To investigate size and shape of bismuth oxide nanoparticles, field emission scanning electron microscope (FE-SEM) employed by using a MIRA-TESCAN. To evaluate cross-linked chitosan-coated bismuth oxide nanoparticles, FTIR spectroscopy was performed by using a Frontier PerkinElmer spectrometer.

2.4. CT imaging: To evaluate the behaviour of chitosan-coated bismuth oxide nanoparticles as a CT contrast agent, an X-ray attenuation experiment was performed according to Abdomen protocol. To determine image resolution enhancement in the case of using chitosan-coated bismuth oxide nanoparticles as a contrast agent, the experiment was carried out for a commercial iodinated contrast agent (Iohexol, Omnipaque) additionally. To enhance results reliability, both bismuth oxide nanoparticles and Iohexol were harnessed in identical concentrations. The assay has carried out at the Bi_2O_3 nanoparticles concentration of 1, 2, 3, 4, 5 and 6 mg/ml and all samples were poured in 2 ml microtubes. Eventually, a CT scanner (GE Healthcare) with an X-ray voltage of 80 keV was used to obtain the CT images.

2.5. In vitro studies – MTT assay: To evaluate the cytotoxicity of chitosan-coated bismuth oxide nanoparticles, the MTT-based assay was carried out based on the described protocol [52]. In this regard, the cytotoxicity of the modified nanoparticles carried out on the HDF-1 cell line derived from the dermis of the normal human neonatal foreskin or adult skin. The mentioned cell line was purchased from Iranian Biological Resource Center (Tehran, Iran). These cells were conveyed to 200 µl high glucose Dulbecco's modified Eagle's medium 5 (DMEM) including 10% foetal bovine serum (FBS) in a 96-well microtitration plate and the seeding density per each well was 5000 cells. The incubated period was initiated by adding different concentrations (1, 2.5, 5, 10 and 20 ppm) of chitosan-coated bismuth oxide nanoparticles when the mentioned cells arrived at the logarithmic phase of growth after 3 days. To obtain reliable results, the procedure was repeated three times. This process has been carried out for both chitosan-coated bismuth oxide nanoparticle and bismuth oxide nanoparticles without surface modification. After 72 h, bismuth oxide nanoparticles were effaced from the wells. Recovery period contemplated 3 days in order to demonstrate the regenerative capacity of survived exposed cells. After this stage, fresh medium was exploited to nourish the plates every day. Afterwards, the medium in each well was discarded and then 200 µl DMEM without FBS beside 50 µl of MTT solution (5 mg/ml) was added to all wells at the termination of the recovery period and the plates were additionally incubated for 4 h. After that, all remnant supernatants were removed. Thence, 200 µl of dimethyl sulphoxide

doi: 10.1049/mnl.2018.5145

was added to solve insoluble formazan crystals. Thereupon, 25 µl of glycine buffer was added to all wells to adjust the ultimate pH. Afterwards, a microtitration plate reader (BioTek®, USA) was employed to record absorbance at a certain wavelength (570 nm). The absolute standards of the absorbance altered to living portion data as the percentage of surviving cells of the control.

3. Results and discussion

3.1. Morphological, structural and optical properties: To evaluate the shape and size distribution of prepared Bi_2O_3 nanoparticles, FE-SEM was employed. Fig. 1 shows spherical-shaped Bi_2O_3 nanoparticles in the range of 10–75 nm. To determine the average size and related distribution of synthesised nanoparticles, more than 500 nanoparticles were considered. As it can be seen in Fig. 1, the average size of 40 ± 20 nm was obtained. Although a specific current was used to prepare Bi_2O_3 nanoparticles via EAD in this study, the size and shape of Bi_2O_3 nanoparticles can be controlled via regulating electric current and synthesis medium variation [35, 53].

To characterise synthesised Bi_2O_3 nanoparticles, UV-vis spectroscopy was carried out to confirm Bi_2O_3 nanoparticles formation initially. In addition, optical measurement demonstrates Bi_2O_3 nanoparticles stability and probable agglomeration during the time. In this regard, the optical transmission spectra of Bi and Bi_2O_3 nanoparticles solution measured between 190 and 800 nm wavelengths and an absorbance peak observed at 273 nm wavelength shown in Fig. 2. It demonstrates the formation of Bi_2O_3 nanoparticles has been revealed in previous studies [34, 54, 55].

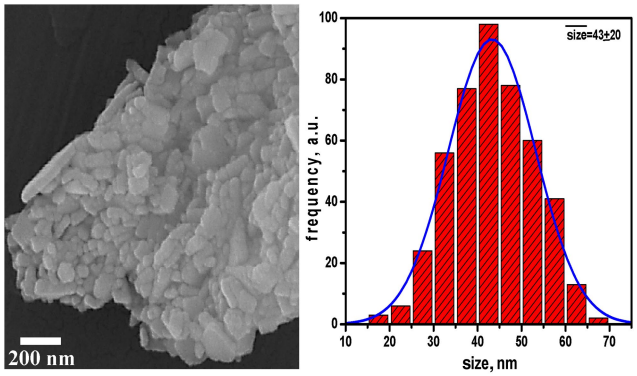

Fig. 1 *FE-SEM image of bismuth oxide nanoparticles and their size distribution*

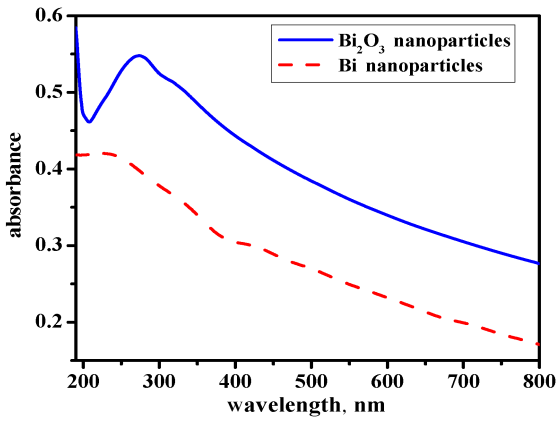

Fig. 2 *UV-vis spectra of synthesised bismuth and bismuth oxide nanoparticles*

Then, to evaluate the phase and crystalline structure of synthesised Bi_2O_3 nanoparticles, XRD analysis was performed. The presented XRD pattern in Fig. 3 confirms the formation of Bi_2O_3 and hydroxide bismuth phases. The crystalline system of formed Bi_2O_3 is monoclinic and dimensions are $a = 5.83$, $b = 8.14$ and $c = 7.48$A°, as well as, α, β and γ are 90°, 67° and 90°, respectively. Furthermore, the diffraction peaks of monoclinic Bi_2O_3 nanocrystals are observed at $2\theta = 24.6$, 25.8, 32.6, 40.2, 42.1, 46.5, 52.1, 56, 62.7, 65.6,.7 and 84.7°, which, respectively, are related to (102), (002), (211), (220), (211), (223), (003), (240), (104), (251), (134) and (342) planes according to the JCPDS Card No. 01-072-0398. Besides, because of the long lasting existence of Bi_2O_3 nanoparticles in water medium according to the synthesis approach type, the bismuth hydroxide $Bi(OH)_3$ was also observed.

The FTIR spectroscopy clarifies bands' variations during a certain process. To investigate the bands of Bi_2O_3 nanoparticles solutions with and without chitosan, and to confirm cross-linked chitosan via GTA around the Bi_2O_3 nanoparticles, the FTIR spectroscopy of chitosan, Bi_2O_3 nanoparticles, and chitosan-coated Bi_2O_3 was carried out. As shown in Fig. 4, in the chitosan spectrum, the peaks at 1079, 1379 and 2879 cm^{-1} are related to C–O, C–N, and C–H bands, respectively. Furthermore, the peak at 3380 cm^{-1} is related to O–N and N–H bands [56]. In the Bi_2O_3–$Bi(OH)_3$ spectra, the peak at 844 cm^{-1} is related to the Bi–O band and peaks at 1390 and 1480 cm^{-1} are related to the C–H band [56, 57]. In the chitosan-coated Bi_2O_3 nanoparticles spectra, the peak at 1074 cm^{-1} is attributed to the C–O stretching band. The

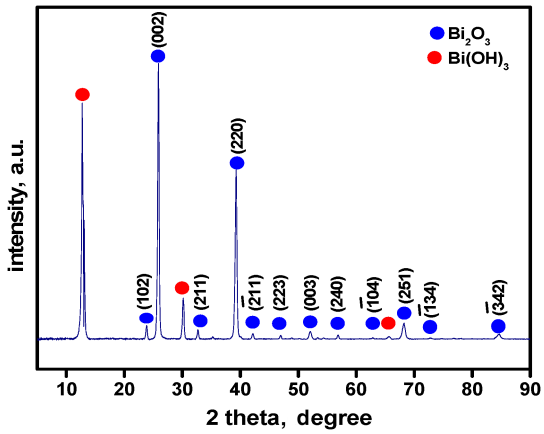

Fig. 3 *XRD results of bismuth oxide and bismuth hydroxide*

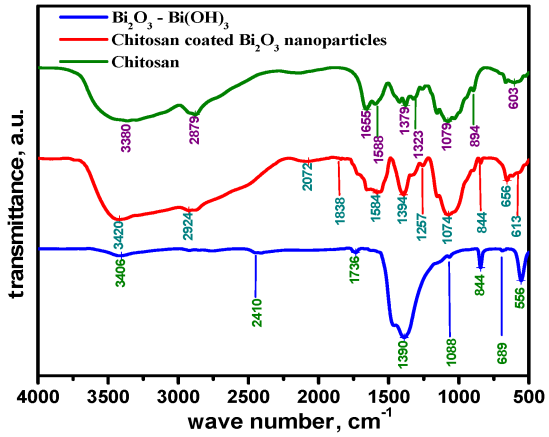

Fig. 4 *FTIR spectra of bismuth oxide nanoparticles with and without chitosan*

sharp peaks at 1394 and 1585 cm^{-1} are allocated to C–N and stretching aromatic C=C band, respectively [58]. Moreover, the peak at 1660 cm^{-1} belongs to the imine group formation. Finally, the peaks at 2924 are 3420 cm^{-1} attributed to the C–H band and the stretching band of N–H or OH of chitosan, successively [59]. In chitosan-coated Bi_2O_3 nanoparticles spectra, there are two shifts in comparison with Bi_2O_3 nanoparticles at 844 and 556 cm^{-1}. These variations confirm converting the chitosan N–H amino group into the C=N imine group at 1670 cm^{-1}, which implies cross-linking chitosan via GTA [58].

3.2. CT imaging: In this study, the feasibility of chitosan-coated Bi_2O_3 nanoparticles as a contrast agent for X-ray CT has been investigated. In this regard, the CT imaging of chitosan-coated Bi_2O_3 nanoparticles (the concentrations of 1, 2, 3, 4, 5 and 6 mg/ml) was performed according to the abdomen protocol and voltage of 80 keV was applied. Moreover, the CT contrast of Iohexol, a commercial CT contrast agent, was evaluated in the same concentrations and conditions. Fig. 5 shows the CT contrast of chitosan-coated Bi_2O_3 nanoparticles and Iohexol.

As predicted, by increasing chitosan-coated Bi_2O_3 nanoparticles concentrations, X-ray attenuation increased. A similar behaviour was observed for Iohexol too. The CT numbers of chitosan-coated Bi_2O_3 nanoparticles were 16, 30, 49, 66, 75 and 85 in the concentrations of 1, 2, 3, 4, 5 and 6 mg/ml successively. On the contrary, the related X-ray attenuation results for commercial Iohexol were 5, 14, 25, 34, 44 and 57. By comparing X-ray attenuation of chitosan-coated Bi_2O_3 nanoparticles and Iohexol, it can be seen that the CT number of chitosan-coated Bi_2O_3 nanoparticles is higher than Iohexol in identical concentrations. The X-ray attenuation difference of chitosan-coated Bi_2O_3 nanoparticles and Iohexol is not much at lower concentrations and by increasing concentrations the CT number variation increased. By and large, the results demonstrate that chitosan-coated Bi_2O_3 nanoparticles are an appropriate contrast agent for X-ray CT and are competitive with a commercial Iohexol contrast agent.

3.3. In vitro studies: To investigate cell cytotoxicity of chitosan-coated Bi_2O_3 nanoparticles, the MTT-based assay was carried out on the HDF-1 cell line.

The study was performed on various concentrations of chitosan-coated Bi_2O_3 nanoparticles (1, 2.5, 5, 10 and 20 ppm). Fig. 6 shows the cell viability values of the HDF-1 cell line versus concentration of chitosan-coated Bi_2O_3 nanoparticles. As seen in Fig. 6, by increasing chitosan-coated Bi_2O_3 nanoparticles concentration, cell viability decreases from 96 to 80%. Moreover, there is a considerable non-toxicity in all concentrations. In addition, it was reported that chitosan coating leads to reduced toxicity of metal

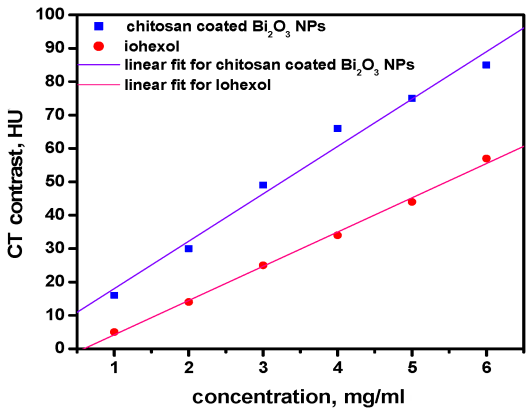

Fig. 5 *CT value (HU) of chitosan-coated Bi_2O_3 nanoparticles and Iohexol in various concentrations at a voltage of 80 keV*

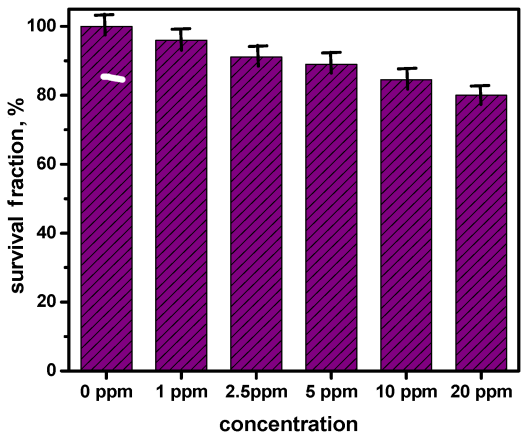

Fig. 6 *Cell cytotoxicity evaluation of Bi_2O_3 nanoparticles on HDF-1 cell line*

oxide nanoparticles [15]. Therefore, the chitosan-coated Bi_2O_3 nanoparticles are suitable for in vitro and in vivo studies and applications.

4. Conclusion: Bi_2O_3 nanoparticles synthesised via the EAD approach in a water medium and 5 A current. UV-vis spectroscopy demonstrated the Bi_2O_3 nanoparticles absorbance peak at 273 nm and the XRD pattern confirmed the monoclinic structure formation. The FE-SEM images displayed the average size of spherical nanoparticles of 40 nm. The FTIR spectra showed peaks at 1584 and 1660 cm^{-1} that are related to the C=N imine bond and C=C ethylenic bond, respectively, which demonstrated the reaction of chitosan with GTA. The cell cytotoxicity of chitosan-coated Bi_2O_3 nanoparticles on the HDF-1 cell line displayed no considerable toxicity. The CT number of chitosan-coated Bi_2O_3 nanoparticles increased via concentration increment (16, 30, 49, 66, 75 and 85 at concentrations of 1, 2, 3, 4, 5 and 6 mg/ml). Moreover, the X-ray attenuation results demonstrated Iohexol samples CT numbers 5, 14, 25, 34, 44 and 57 at the same concentrations. As is seen, the X-ray attenuation of chitosan-coated Bi_2O_3 nanoparticles in comparison with commercial Iohexol is higher and all concentrations and variation increase by an increase in concentration. Finally, the results showed that chitosan-coated Bi_2O_3 nanoparticles are an appropriate candidate for the X-ray CT contrast agent.

5 References

[1] Lusic H., Grinstaff M.W.: 'X-ray-computed tomography contrast agents', *Chem. Rev.*, 2012, **113**, (3), pp. 1641–1666

[2] Shilo M., Reuveni T., Motiei M., *ET AL.*: 'Nanoparticles as computed tomography contrast agents: current status and future perspectives', *Nanomedicine*, 2012, **7**, (2), pp. 257–269

[3] Hyafil F., Cornily J.-C., Feig J.E., *ET AL.*: 'Noninvasive detection of macrophages using a nanoparticulate contrast agent for computed tomography', *Nat. Med.*, 2007, **13**, (5), p. 636

[4] Yin Q., Yap F.Y., Yin L., *ET AL.*: 'Poly (iohexol) nanoparticles as contrast agents for in vivo X-ray computed tomography imaging', *J. Am. Chem. Soc.*, 2013, **135**, (37), pp. 13620–13623

[5] He W., Ai K., Lu L.: 'Nanoparticulate X-ray CT contrast agents', *Sci. China Chem.*, 2015, **58**, (5), pp. 753–760

[6] Cormode D.P., Naha P.C., Fayad Z.A.: 'Nanoparticle contrast agents for computed tomography: a focus on micelles', *Contrast Media Mol. Imaging*, 2014, **9**, (1), pp. 37–52

[7] Jakhmola A., Anton N., Vandamme T.F.: 'Inorganic nanoparticles based contrast agents for X-ray computed tomography', *Adv. Healthcare Mater.*, 2012, **1**, (4), pp. 413–431

[8] Yu S.-B., Watson A.D.: 'Metal-based X-ray contrast media', *Chem. Rev.*, 1999, **99**, (9), pp. 2353–2378

doi: 10.1049/mnl.2018.5145

[9] Cole L.E., Ross R.D., Tilley J.M., *et al.*: 'Gold nanoparticles as contrast agents in X-ray imaging and computed tomography', *Nanomedicine*, 2015, **10**, (2), pp. 321–341

[10] Taupin F., Flaender M., Delorme R., *et al.*: 'Gadolinium nanoparticles and contrast agent as radiation sensitizers', *Phys. Med. Biol.*, 2015, **60**, (11), p. 4449

[11] Liu Y., Ai K., Liu J., *et al.*: 'A high-performance ytterbium-based nanoparticulate contrast agent for in vivo x-ray computed tomography imaging', *Angew. Chem., Int. Ed.*, 2012, **51**, (6), pp. 1437–1442

[12] Brown A.L., Goforth A.M.: 'pH-dependent synthesis and stability of aqueous, elemental bismuth glyconanoparticle colloids: potentially biocompatible x-ray contrast agents', *Chem. Mater.*, 2012, **24**, (9), pp. 1599–1605

[13] Tan L., Liu T., Fu C., *et al.*: 'Hollow ZrO_2/PPy nanoplatform for improved drug delivery and real-time CT monitoring in synergistic photothermal-chemo cancer therapy', *J. Mater. Chem. B*, 2016, **4**, (5), pp. 859–866

[14] Torres A.S., Bonitatibus P.J.Jr., Colborn R.E., *et al.*: 'Biological performance of a size-fractionated core-shell tantalum oxide nanoparticle x-ray contrast agent', *Invest. Radiol.*, 2012, **47**, (10), pp. 578–587

[15] Firouzi M., Poursalehi R., Delavari H., *et al.*: 'Chitosan coated tungsten trioxide nanoparticles as a contrast agent for X-ray computed tomography', *Int. J. Biol. Macromol.*, 2017, **98**, pp. 479–485

[16] Ai K., Liu Y., Liu J., *et al.*: 'Large-scale synthesis of Bi_2S_3 nanodots as a contrast agent for in vivo X-ray computed tomography imaging', *Adv. Mater.*, 2011, **23**, (42), pp. 4886–4891

[17] Au J.T., Craig G., Longo V., *et al.*: 'Gold nanoparticles provide bright long-lasting vascular contrast for CT imaging', *Am. J. Roentgenol.*, 2013, **200**, (6), pp. 1347–1351

[18] Detappe A., Thomas E., Tibbitt M.W., *et al.*: 'Ultrasmall silica-based bismuth gadolinium nanoparticles for dual magnetic resonance-computed tomography image guided radiation therapy', *Nano Lett.*, 2017, **17**, (3), pp. 1733–1740

[19] Zheng X., Wang Y., Sun L., *et al.*: 'Tbf_3 nanoparticles as dual-mode contrast agents for ultrahigh field magnetic resonance imaging and X-ray computed tomography', *Nano Res.*, 2016, **9**, (4), pp. 1135–1147

[20] Vega-Jiménez A., Almaguer-Flores A., Flores-Castañeda M., *et al.*: 'Bismuth subsalicylate nanoparticles with anaerobic antibacterial activity for dental applications', *Nanotechnology*, 2017, **28**, (43), p. 435101

[21] Abudayyak M., Öztaş E., Arici M., *et al.*: 'Investigation of the toxicity of bismuth oxide nanoparticles in various cell lines', *Chemosphere*, 2017, **169**, pp. 117–123

[22] Cheng X., Yong Y., Dai Y., *et al.*: 'Enhanced radiotherapy using bismuth sulfide nanoagents combined with photo-thermal treatment', *Theranostics*, 2017, **7**, (17), p. 4087

[23] Deng J., Xu S., Hu W., *et al.*: 'Tumor targeted, stealthy and degradable bismuth nanoparticles for enhanced X-ray radiation therapy of breast cancer', *Biomaterials*, 2018, **154**, pp. 24–33

[24] Brown A.L., Naha P.C., Benavides-Montes V., *et al.*: 'Synthesis, X-ray opacity, and biological compatibility of ultra-high payload elemental bismuth nanoparticle X-ray contrast agents', *Chem. Mater.*, 2014, **26**, (7), pp. 2266–2274

[25] Kowalik M., Masternak J., Barszcz B.: 'Recent research trends on bismuth compounds in cancer chemo-and radiotherapy', *Curr. Med. Chem.*, 2017

[26] Zhou D., Li C., He M., *et al.*: 'Folate-targeted perfluorohexane nanoparticles carrying bismuth sulfide for use in US/CT dual-mode imaging and synergistic high-intensity focused ultrasound ablation of cervical cancer', *J. Mater. Chem. B*, 2016, **4**, (23), pp. 4164–4181

[27] Lu Q., Gao F., Komarneni S.: 'Biomolecule-assisted synthesis of highly ordered snowflakelike structures of bismuth sulfide nanorods', *J. Am. Chem. Soc.*, 2004, **126**, (1), pp. 54–55

[28] Borglin J., Selegård R., Aili D., *et al.*: 'Peptide functionalized gold nanoparticles as a stimuli responsive contrast medium in multiphoton microscopy', *Nano Lett.*, 2017, **17**, (3), pp. 2102–2108

[29] Dadashi S., Poursalehi R., Delavari H. H.: 'In situ PEGylation of Bi nanoparticles prepared via pulsed Nd: YAG laser ablation in low molecular weight PEG: a potential X-ray CT imaging contrast agent', *Comput. Methods Biomech. Biomed. Eng. Imaging Vis.*, 2018, pp. 1–8, doi: 10.1080/21681163.2018.1452634

[30] Nazari P., Dowlatabadi-Bazaz R., Mofid M., *et al.*: 'The antimicrobial effects and metabolomic footprinting of carboxyl-capped bismuth nanoparticles against *Helicobacter pylori*', *Appl. Biochem. Biotechnol.*, 2014, **172**, (2), pp. 570–579

[31] Li Z., Hu Y., Howard K.A., *et al.*: 'Multifunctional bismuth selenide nanocomposites for antitumor thermo-chemotherapy and imaging', *ACS Nano*, 2015, **10**, (1), pp. 984–997

[32] Liu J., Zheng X., Yan L., *et al.*: 'Bismuth sulfide nanorods as a precision nanomedicine for in vivo multimodal imaging-guided photothermal therapy of tumor', *ACS Nano*, 2015, **9**, (1), pp. 696–707

[33] Pan C., Li X., Wang F., *et al.*: 'Synthesis of bismuth oxide nanoparticles by the polyacrylamide gel route', *Ceram. Int.*, 2008, **34**, (2), pp. 439–441

[34] Dadashi S., Poursalehi R.: 'Formation, gradual oxidation mechanism and tunable optical properties of Bi/Bi_2O_3 nanoparticles prepared by Nd: YAG laser ablation in liquid: dissolved oxygen as genesis of tractable oxidation', *Mater. Res. Bull.*, 2018, **97**, pp. 421–427

[35] Ziashahabi A., Poursalehi R., Naseri N.: 'Formation mechanism of bead-chain-like ZnO nanostructures from oriented attachment of Zn/ZnO nanocomposites prepared via DC arc discharge in liquid', *Mater. Sci. Semicond. Process.*, 2017, **72**, pp. 128–133

[36] Ashkarran A.A., Mahdavi S.M., Ahadian M.M.: 'ZnO nanoparticles prepared by electrical arc discharge method in water', *Mater. Chem. Phys.*, 2009, **118**, (1), pp. 6–8

[37] Lange H., Sioda M., Huczko A., *et al.*: 'Nanocarbon production by arc discharge in water', *Carbon*, 2003, **41**, (8), pp. 1617–1623

[38] Ashkarran A., Ahadian M., Ardakani S.M.: 'Synthesis and photocatalytic activity of WO3 nanoparticles prepared by the arc discharge method in deionized water', *Nanotechnology*, 2008, **19**, (19), p. 195709

[39] Lung J.-K., Huang J.-C., Tien D.-C., *et al.*: 'Preparation of gold nanoparticles by arc discharge in water', *J. Alloys Compd.*, 2007, **434**, pp. 655–658

[40] Groult H., Poupard N., Herranz F., *et al.*: 'Family of bioactive heparin-coated iron oxide nanoparticles with positive contrast in magnetic resonance imaging for specific biomedical applications', *Biomacromolecules*, 2017, **18**, (10), pp. 3156–3167

[41] Peng X.-H., Qian X., Mao H., *et al.*: 'Targeted magnetic iron oxide nanoparticles for tumor imaging and therapy', *Int. J. Nanomed.*, 2008, **3**, (3), p. 311

[42] Sun I.-C., Na J.H., Jeong S.Y., *et al.*: 'Biocompatible glycol chitosan-coated gold nanoparticles for tumor-targeting CT imaging', *Pharm. Res.*, 2014, **31**, (6), pp. 1418–1425

[43] Chen Q., Wang H., Liu H., *et al.*: 'Multifunctional dendrimer-entrapped gold nanoparticles modified with RGD peptide for targeted computed tomography/magnetic resonance dual-modal imaging of tumors', *Anal. Chem.*, 2015, **87**, (7), pp. 3949–3956

[44] Paul P., Sengupta S., Mukherjee B., *et al.*: 'Chitosan-coated nanoparticles enhanced lung pharmacokinetic profile of voriconazole upon pulmonary delivery in mice', *Nanomedicine*, 2018, **13**, (5), pp. 501–520

[45] Wei H., Lai S., Wei J., *et al.*: 'A novel delivery method of cyclovirobuxine D for brain-targeting: chitosan coated nanoparticles loading cyclovirobuxine D by intranasal administration', *J. Nanosci. Nanotechnol.*, 2018, **18**, (8), pp. 5274–5282

[46] Ali A., Ahmed S.: 'A review on chitosan and its nanocomposites in drug delivery', *Int. J. Biol. Macromol.*, 2017, **109**, (2017), pp. 273–286

[47] Usman A., Zia K.M., Zuber M., *et al.*: 'Chitin and chitosan based polyurethanes: A review of recent advances and prospective biomedical applications', *Int. J. Biol. Macromol.*, 2016, **86**, pp. 630–645

[48] Vunain E., Mishra A., Mamba B.: 'Fundamentals of chitosan for biomedical applications' in 'Chitosan based biomaterials, South Africa, volume 1' (Elsevier, 2017), pp. 3–30

[49] Vaz J., Pezzoli D., Chevallier P., *et al.*: 'Antibacterial coatings based on chitosan for pharmaceutical and biomedical applications', *Curr. Pharm. Des.*, 2018, **24**, (8), pp. 866–885

[50] Ahsan S.M., Thomas M., Reddy K.K., *et al.*: 'Chitosan as biomaterial in drug delivery and tissue engineering', *Int. J. Biol. Macromol.*, 2017, **110**, (2017), pp. 97–109

[51] Radhakumary C., Nair P.D., Reghunadhan Nair C., *et al.*: 'Chitosan-graft-poly (vinyl acetate) for hemodialysis applications', *J. Appl. Polym. Sci.*, 2012, **125**, (3), pp. 2022–2033

[52] Sadighi S., Amanpour S., Behrouzi B., *et al.*: 'Lack of metformin effects on different molecular subtypes of breast cancer under normoglycemic conditions: an in vitro study', *Asian Pac. J. Cancer Prev.*, 2014, **15**, (5), pp. 2287–2290

[53] Keidar M.: 'Factors affecting synthesis of single wall carbon nanotubes in arc discharge', *J. Phys. D: Appl. Phys.*, 2007, **40**, (8), p. 2388

[54] Raza W., Haque M., Muneer M., *ET AL.*: 'Synthesis, characterization and photocatalytic performance of visible light induced bismuth oxide nanoparticle', *J. Alloys Compd.*, 2015, **648**, pp. 641–650
[55] Gumus G., Filik H., Demirata B.: 'Determination of bismuth and zinc in pharmaceuticals by first derivative UV–visible spectrophotometry', *Anal. Chim. Acta*, 2005, **547**, (1), pp. 138–143
[56] Ward A.J., Rich A.M., Masters A.F., *ET AL.*: 'Unprecedented blue-shift in bismuth oxide supported on mesoporous silica', *New J. Chem.*, 2013, **37**, (3), pp. 593–600
[57] Kulkarni V., Kulkarni P., Keshavayya J.: 'Glutaraldehyde-crosslinked chitosan beads for controlled release of diclofenac sodium', *J. Appl. Polym. Sci.*, 2007, **103**, (1), pp. 211–217
[58] Monteiro O.A.Jr., Airoldi C.: 'Some studies of crosslinking chitosan–glutaraldehyde interaction in a homogeneous system', *Int. J. Biol. Macromol.*, 1999, **26**, (2–3), pp. 119–128
[59] Ibrahim M., Osman O., Mahmoud A.A.: 'Spectroscopic analyses of cellulose and chitosan: FTIR and modeling approach', *J. Comput. Theor. Nanosci.*, 2011, **8**, (1), pp. 117–123

doi: 10.1049/mnl.2018.5145